



Heriot-Watt University
Research Gateway

Validation of a blood plasma separation system by biomarker detection

Citation for published version:

Kersaudy-Kerhoas, M, Kavanagh, DM, Dhariwal, RS, Campbell, CJ & Desmulliez, MPY 2010, 'Validation of a blood plasma separation system by biomarker detection', *Lab on a Chip*, vol. 10, no. 12, pp. 1587-1595. <https://doi.org/10.1039/b926834k>

Digital Object Identifier (DOI):

[10.1039/b926834k](https://doi.org/10.1039/b926834k)

Link:

[Link to publication record in Heriot-Watt Research Portal](#)

Document Version:

Publisher's PDF, also known as Version of record

Published In:

Lab on a Chip

General rights

Copyright for the publications made accessible via Heriot-Watt Research Portal is retained by the author(s) and / or other copyright owners and it is a condition of accessing these publications that users recognise and abide by the legal requirements associated with these rights.

Take down policy

Heriot-Watt University has made every reasonable effort to ensure that the content in Heriot-Watt Research Portal complies with UK legislation. If you believe that the public display of this file breaches copyright please contact open.access@hw.ac.uk providing details, and we will remove access to the work immediately and investigate your claim.

Validation of a blood plasma separation system by biomarker detection

Maiwenn Kersaudy-Kerhoas,^{*a} Deirdre M. Kavanagh,^a Resham S. Dhariwal,^a Colin J. Campbell^{bc} and Marc P. Y. Desmulliez^a

Received 22nd December 2009, Accepted 3rd March 2010

First published as an Advance Article on the web 31st March 2010

DOI: 10.1039/b926834k

A microfluidic system was developed for blood plasma separation at high flow rate. This system uses only hydrodynamic forces to separate plasma from whole blood. The microfluidic network features a series of constrictions and bifurcations to enhance the product yield and purity. A maximum purity efficiency of 100% is obtained on blood with entrance hematocrit level up to 30% with a flow rate of 2 mL h⁻¹. Flow cytometry was performed on the extracted plasma to evaluate the separation efficiency and to assess cell damage. A core target of this study was the detection of cell-free DNA from the on-chip extracted plasma. To this effect, PCR was successfully carried out off-chip on the cell-free DNA present in the plasma extracted on-chip. A house-keeping gene sequence (GAPDH) was amplified without the need for a purification after the separation, thereby showing the high quality of the plasma sample. The resulting data suggests that the system can be used as a preliminary module of a total analysis system for cell-free DNA detection in human plasma.

Introduction

Blood plasma separation on-chip

Optimum on-chip blood plasma separation techniques should have a large throughput, a high plasma yield and purity, with minimum cellular damage in order to prevent contamination of the plasma with cellular DNA and haemoglobin. In that respect, several broad avenues of research have been implemented that try to replicate the benefits of traditional centrifugation methods. The miniaturisation of centrifugation has been the topic of many research groups. Ducrée and Madou, for example, have utilised centrifugal forces developed through the rotation of their lab-on-CD devices to separate red blood cells from plasma.^{1,2} Among the advantages of the lab-on-CD platform is the lack of clogging effect that might reduce the efficiency of separation in other devices. Centrifugation is often considered as “non-continuous”, however on Lab-on-CD devices, the samples might be processed in-line after the separation or other functions.³ Filtration is another conventional method to separate plasma from whole blood, and has also been miniaturised. Moorthy *et al.* presented a device with an integrated membrane, or porous plug, allowing the filtration of cells greater than 3 µm, however the device is easily clogged.⁴ Cross-flow filtration has been implemented with more success by Vandelinder *et al.* and Chen *et al.* in polydimethylsiloxane (PDMS) devices.^{5,6} However, as pointed out by

Becker, results obtained in PDMS devices are hardly reproducible for commercial chip applications.⁷

Some researchers have focused on the development of more continuous separation methods applicable to blood plasma separation using hydrodynamic forces. These methods, alongside centrifugal and filtration techniques, are sometimes labelled as “passive”, as they do not require any external force field but the force induced by the pumping of the fluid itself.⁸ Yang *et al.* developed a microfluidic network with a series of 10 µm bifurcations in a 15 µm main channel.⁹ The same principle was used by Fan *et al.* to extract plasma for protein analysis.¹⁰ Faivre has used constrictions integrated before a bifurcation to increase the natural cell-free layer of blood flow at low Reynolds number using lateral migration.¹¹ Lateral migration has also been demonstrated to extract plasma at higher Reynolds number and large flow rate by Di Carlo.¹² An exhaustive comparison of passive blood plasma separation techniques has been presented by Sollier *et al.*⁸ More recently, Rodríguez-Villarreal *et al.* have demonstrated a high flow rate blood plasma separation device using one constriction and one bifurcation.¹³ The biological validation of the resulting extracted plasma in terms of contamination was not however presented in this article. Additionally, active blood plasma separation may be performed using dielectrophoretic, acoustic or magnetic forces.¹⁴

In this paper we present a blood plasma extraction microsystem based on multiple constrictions in a microfluidic network together with the biological validation of this device through the detection of human cell free DNA (cfDNA) in the extracted plasma. The chip overcomes certain limitations encountered in the literature as it runs at high-flow rate, high throughput, and produces a substantial amount of pure plasma while causing very little cellular damage allowing thereby the extracted plasma to be suitable for detection of cfDNA. In this regard, our microfluidic plasma separator can be regarded as a preliminary module to a low cost total analysis system for these types of applications.^{15,16}

^aMicroSystems Engineering Centre (MISEC), School of Engineering & Physical Sciences, Heriot-Watt University, Earl Mountbatten Building, Edinburgh, United Kingdom. E-mail: mk87@hw.ac.uk; Fax: +44 131 451 4155; Tel: +44 131 451 4148

^bDivision of Pathway Medicine, University of Edinburgh Medical School, Chancellor's Building, 49 Little France Crescent, Edinburgh, United Kingdom. E-mail: colin.campbell@ed.ac.uk; Fax: +44 131 242 6244; Tel: +44 131 242 6242

^cSchool of Chemistry, University of Edinburgh, Joseph Black building, West Mains road, Edinburgh, United Kingdom EH9 3JJ. E-mail: colin.campbell@ed.ac.uk; Fax: +44 131 650 6453; Tel: +44 131 650 7546

cfDNA

The existence of cell free DNA (cfDNA) in human plasma was first detected in cancer patients over 30 years ago.¹⁷ However only in the last few years has its true diagnostic potential been realised resulting in an increasing interest in the detection and analysis of cfDNA.^{18–21} Potential applications of cfDNA detection include the diagnosis and prognosis of various malignancies,^{18,19,21,22} the monitoring of graft *versus* host disease after organ transplantation²³ and non-invasive prenatal diagnosis (NIPD).²⁴ For the latter, cell free foetal DNA, cffDNA, is not only used today to diagnose gender-linked conditions²⁵ or foetal rhesus D status^{26,27} but cffDNA is also employed as an indicator for pregnancy associated diseases such as pre-eclampsia and preterm labour.²⁸

Biology of cfDNA

cfDNA exists as small fragments of DNA typically of less than 450 bp. The origin of cfDNA in blood is not fully understood but is believed to be related to the cellular processes of necrosis and apoptosis. Evidence to support the latter mechanism is seen in cancer patients where, in some cases, cfDNA has been shown to have the typical apoptotic ladder profile associated with the inter-nucleosome cleavage of genomic DNA.²⁹ On the other hand, the former mechanism proposes that cfDNA is released by macrophages after phagocytosis of necrotic cells.¹¹ Another proposal suggests that DNA could also be released by the lysis of intact cancer or foetal cells after they enter the blood stream. Multiple studies have shown that, during pregnancy, the major source of cffDNA is believed to be the placenta.^{30–32} In healthy individuals cfDNA concentration in blood is between 0 and 100 ng ml⁻¹, with a mean value of 30 ng ml⁻¹.³³ Cancer patients have higher levels of cfDNA often with averages of 180 ng ml⁻¹,³² most of this DNA is double stranded in its nucleoprotein form.³⁴ cffDNA is also believed to be protected within apoptotic bodies or associated with nucleosomes.³⁵ The mean fractional concentrations of cffDNA in early and late pregnancy are 3.4% and 6.2% in plasma, respectively, and 0.13% and 1% in serum. A higher background of maternal DNA is found in serum believed to be released by clot formation.^{36,37}

Analysis of cfDNA from plasma by PCR

Analysis of cfDNA first requires the separation of plasma or serum from whole blood. Purification is mostly required to remove the major inhibitors of the Polymerase Chain Reaction (PCR). These include natural components such as heme and immunoglobulin G and exogenous components such as anticoagulants.³⁸ Furthermore, the plasma must be completely free of cells, reducing thereby the contamination of the plasma with cellular DNA which can interfere with the accuracy of the DNA analysis. Traditionally plasma is separated from blood by centrifugation or filtration. For the preparation of cfDNA an additional step of filtration or micro-centrifugation is often recommended to ensure that the plasma or serum is of a high purity.³⁹ The DNA may be further purified by extraction before performing PCR. As yet there are no officially agreed standards for the purification of DNA from plasma, but the most common and fastest method is the QIAamp blood kit, which uses the

binding of DNA to a silica-gel membrane. Some studies claim however a 20% less recovery of cfDNA using this kit compared to other methods of DNA purification such as the Triton/Heat/Phenol (THP) protocol.⁴⁰

cfDNA loss during purification has been reported to occur due to the small fragment size.⁴¹ These processing steps although necessary can also be slow and cumbersome. Moreover the generation of aerosols is common during centrifugation, which can be a potential risk of infection and contamination. Cell damage and cell loss is also a concern during centrifugation.⁴² For point-of-care diagnostics, it is also well known that sample preparation step is a serious bottleneck in microfluidics. The development of a miniaturised module capable of de-skilled blood separation would aid in the translation of this new technology.

The objective of this study was to investigate: (i) the influence of the entrance hematocrit and flow rate on the separation efficiency, (ii) the hematocrit and the cell-free zones, (iii) the purity of the plasma obtained using flow cytometry, (iv) the influence of the dilution of whole blood prior to on-chip separation and (v) the influence of the separation efficiency on the PCR efficiency. In order to prove the presence of biomarkers in the extracted plasma and to study the detection limits *versus* dilution levels and purity efficiency, we also performed a series of PCR reactions on human genes.

Theory and design of a blood plasma separator

The number of parameters affecting the flow of cells in a micro-channel renders difficult the prediction of a separation system behaviour. An earlier publication has discussed in detail the presence and effects of viscous and inertial lift forces which enable particles to be separated at the microscale.¹⁵ In a straight microchannel, deformable particles such as leukocytes move away from the walls under either the effect of inertial lift if the Reynolds number is close to 1 or by viscous lift when the Reynolds number is low. Both effects arise from the presence of a stationary wall and the interaction of a shear gradient on the particle. A transitional regime also exists where both effects may co-exist as discussed in ref. 12 and 15. The cell-free layer observed on the walls at certain conditions depends also on the particle-particle interactions and the particle concentration. The design presented here exploits two main hydrodynamic effects: the Zweifach-Fung bifurcation law and the blood flow focusing effect occurring after a constriction. The Zweifach-Fung bifurcation law is an empirical law that addresses the deformable particle behaviour at a bifurcation.⁴³ At a bifurcation, a cell will have the tendency to travel to the daughter channel with the highest flow rate, providing that the cell dimension is comparable to the channel dimension. Although this law was first stated in the context of micro-circulation in the human body, it has also been exploited for *in vitro* separation.⁴³ From a few cells in a microvessel, the law was generalised to accommodate the situation where populations of cells flow in microchannels several tens of microns wide. The Zweifach-Fung effect is commonly used in the design of micro-separators to set up a lower limit for flow rate ratio at a bifurcation.⁹ However, the physics which underpin the law and its limitations are not clearly understood yet. The second effect is the focusing of the flow of

red blood cells after a constriction. In ref. 15, the cell free layer of blood and the focusing of red blood cells after constriction were found to be small in a 200 μm wide microchannel. Faivre *et al.*, reported better focus but used lower Reynolds number and therefore lower flow rate even at higher viscosity.¹¹ In this study we chose to keep the entrance flow rate high, and use inertial lift forces rather than viscous ones.

As shown in Fig. 1, the design bears four connections, a single inlet for whole blood, one outlet for the concentrated cells and two outlets for the extracted plasma. Four plasma channels of 5.5 mm in length are placed on each side of a 100 μm wide main channel at a 45° angle. Meanders are used to minimize the area occupied by the eight plasma channels and keep the footprint of the chip low. A constriction has been placed before each of the plasma channels in order to create a cell-free zone from which the plasma is extracted. A set of chips has 20 μm wide plasma channels while another has 10 μm wide plasma channels. The depth of the microchannel network is 20 μm for all structures.

The plasma channels due to their geometrical features (length and width) have a high fluidic resistance value, whereas the main channel segment which has broader width and shorter length has lower resistance; this difference in resistance value at each bifurcation is proportional to the flow rate ratio. The value of the fluidic resistance of the main channel decreases after each bifurcation. Since the plasma channels have the same lengths the flow rate ratios are expected to be different at each bifurcation. The flow rate ratios can be roughly calculated by the Saber™ Microfluidic applications software (CoventorWare). Flow rate ratios have been calculated as approximately 17.8, 22.6, 31.8 and

55.6 for the left hand side of the chip (bifurcations 1, 3, 5, 7) and 19.2, 25.7, 40.1, and 94.5 for the right hand side of the chip (bifurcations 2, 4, 6, 8) with 20 μm plasma channels. The side having the highest flow rate ratios is expected to perform better. Theoretically, the design should extract 30% of plasma for the 20 μm design and 7% for the 10 μm design.

Materials and methods

Microfluidic chip manufacturing

The microfluidic chips were manufactured by our industrial collaborator, Epigem Ltd (Redcar, UK). The chips consist of several sandwiched layers of the negative photoresist, SU8 between two PMMA layers, ensuring a “whole SU8” channel network. SU8 is patterned using conventional photolithography. Since the chip footprint is small (18 mm \times 23 mm) a generic platform also made from an assembly of PMMA and SU8 is used as a holder featuring standard microfluidic connections (Cheminert) as shown in Fig. 2.

Samples

Human blood was obtained in 500 mL bags from the Scottish National Blood Transfusion Service, Lauriston Place, Edinburgh. Samples were used with the donors' prior consent and ethical clearance was obtained from the SNBTS Sample Governance Committee. Blood was treated with oxalate and stored at 4 °C upon the day of reception. The blood was used

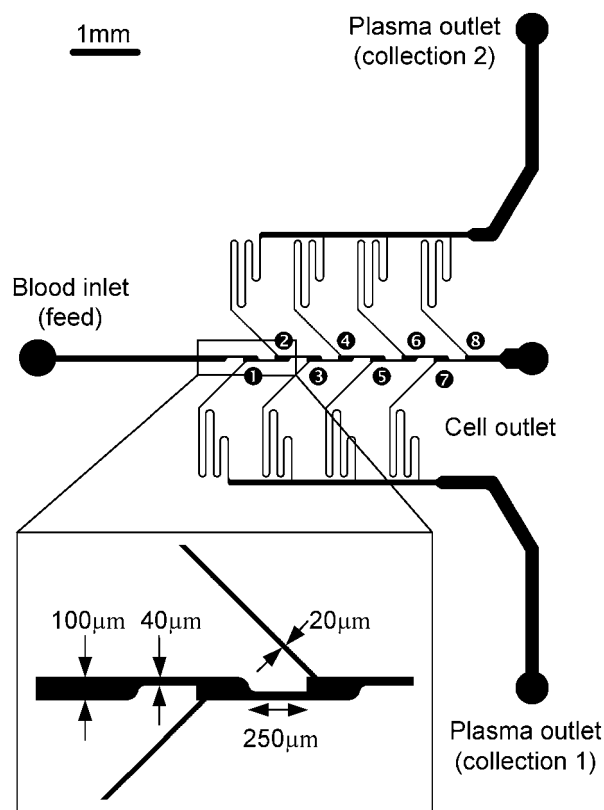


Fig. 1 Blood plasma separation device design. Schematic of a 20 μm wide microchannel blood plasma separator.

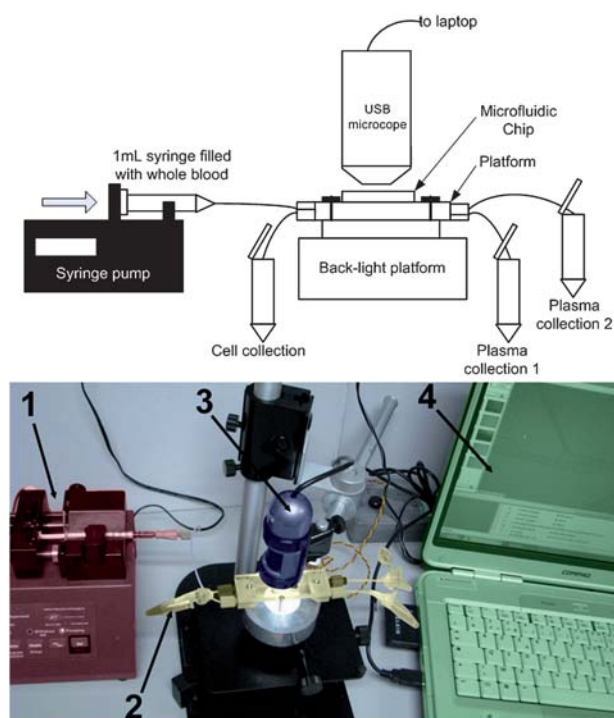


Fig. 2 (a) Schematic of the experimental set-up (*not to scale*). (b) Photograph of experimental set-up: (1) Syringe pump and 1 mL syringe loaded with blood. (2) Blood plasma separation chip device loaded with chip. Eppendorfs on the left collect blood cells, while eppendorfs on the right collect plasma. (3) USB Microscope. (4) Laptop for visualisation.

within a month. Ideally the blood should be separated on the same day, and the PCR performed within hours after the separation. However, this could not be achieved in the current situation. This delay has been taken into account when interpreting the results. During the length of the study two different blood samples were obtained. The blood samples were subjected to different dilutions using Phosphate Buffered Saline, (PBS, Sigma). The dilution levels ranged from zero to 1 : 20. Dilution levels on different blood samples are biased by the intrinsic hematocrit of the blood donor at the time of the collection. Therefore, only resulting hematocrit levels truly reflect the different dilutions performed. Hematocrit level measurements and a full cell count were performed using a Beckman Coulter Counter before each run.

Experimental set-up

The tests were performed at the Division of Pathway Medicine (DPM), University of Edinburgh (Royal Infirmary of Edinburgh, Little France, Edinburgh) in a level II biosafety facility. The chip was loaded onto the holder with microfluidic connections as shown in Fig. 2. The chip and holder assembly was placed onto a custom made back-light apparatus and examined under a digital microscope (DinoLite USB microscope, Big C, USA) to observe the flow and detect any obstacle to the flow path during each experiment. The flow was activated at flow rates ranging from 1 mL h⁻¹ to 10 mL h⁻¹ (from 16.7 μL min⁻¹ to 167 μL min⁻¹) by a syringe pump (Aladdin, WPI, USA). A syringe of 1 mL (BD Plastipak) of blood was loaded for each experiment.

Microfluidic blood plasma separation

Around 50 μL aliquots of each blood sample were placed in individual eppendorf tubes for hematocrit level verification using a Beckman Coulter Counter. The microfluidic devices were pre-filled before each experiment with a 1% BSA-PBS buffer for at least 10 min to avoid cell adhesion during the separation process.⁴⁴ Despite this prevention, the microfluidic network tends to clog up after at least three experiments due to platelets aggregations. If a blockage was spotted or the efficiency of the chip seemed to drop, the chip was discarded and a new one was loaded on the holder. The chips are meant to be low cost and disposable and should really be single-use.

Once the blood samples filled the main channel, the separation process occurred at each bifurcation and the plasma flowed through the individual plasma channels and collection channel. The cell enriched mixture and the extracted plasma were collected in three individual eppendorf tubes, as shown in Fig. 2, and stored at 4 °C until further processing.

Flow cytometry

Staining of the blood sample was performed to label leukocytes and platelets. The R-phycoerythrin (R-PE)- conjugated monoclonal antibody CD45 (PE Mouse Anti-Human, BD Biosciences) was used for leukocytes surface staining. The fluorescein isothiocyanate (FITC)-conjugated CD42 antibodies stained the platelets. Using these markers we were able to identify the leukocytes and platelets population. The RBCs were identified by

being non-stained. Blood cell population analysis was carried out on a FACS Scan instrument (BD Biosciences, San Jose, USA) and results were analysed using Flow Jo software v7.5.3 (Tree Star, Ashland, OR, USA). Determination of the absolute cell count was achieved by the use of flow cytometric beads Flow-Check Fluorospheres (Beckman Coulter). 50 μL of well-mixed beads mixture was added to the 200 μL of sample and mixed thoroughly. The flow cytometer was then calibrated to count a specific number of beads allowing a precise absolute count of the cells.

Amplification of house-keeping gene in the cell-free DNA population present in the plasma extracted on-chip

The amplification primers for the GAPDH gene (forward primer 5'-GAA GGT GAA GGT CGG AGT CA-3', reverse primer 5'-GAC AAG CTT CCC GTT CTC AG) were purchased from Metabion International AG. For the PCR with the GAPDH gene, each reaction aliquot contained 0.4 μM forward primer, 0.4 μM reverse primer, 0.1 μM dNTP (Sigma), 0.1 μM dCTP (Sigma), 2.5 U Taq DNA polymerase (Qiagen HotStarTaq DNA Polymerase kit), 2.5 μL PCR buffer (HotStarTaq DNA Polymerase kit), 4 mM MgCl₂ (Qiagen HotStarTaq DNA Polymerase kit), 9 μL DNA free water. For each reaction, 5 μL of plasma was added to 20 μL of the PCR master mix. In order to determine whether GAPDH could be amplified directly in whole blood, a control consisting of unpurified blood (as received from the blood bank) was measured. As a negative control for PCR, we used ultrapure water. Human genomic control DNA was used as a positive control and was obtained from Promega in 210 ng μL⁻¹ concentration, and diluted at different concentrations.

The thermal cycling program consisted of a 10 min denaturation at 95 °C, followed by 40 cycles of 1 min denaturation at 94 °C, 1 min primer annealing at 68 °C, 1 min extension at 72 °C. The final extension step consisted of a further 5 min cycle at 72 °C and the samples were kept on hold at 10 °C until further processing. The PCR product was purified with the QIAquick PCR purification kit (Qiagen) using the protocol suggested by the manufacturer. The purified DNA product was eluted in 30 μL EB buffer. 10 μL of this product was then loaded onto a 2% agarose gel for analysis by electrophoresis. Gels were analysed using a Biorad Gel Doc system.

Results

Microfluidic plasma extraction

Influence of the entrance hematocrit and flow rate on the separation efficiency. The influence of entrance hematocrit on the separation efficiency was studied using different dilution levels. For the chip with the 20 μm plasma channels, the corresponding hematocrit levels to the dilution levels comprised between 3.3% and 31%. In the chip with the 10 μm plasma channels, higher levels of hematocrit were studied, ranging from 9.4% to 45%. The purity efficiency was defined as:

$$E_p = 1 - \frac{c_p}{c_f}$$

Where c_p and c_f are the number of Red Blood Cells (RBCs) per mL in the plasma collection outlet and in the feed inlet, respectively.

Fig. 3 shows the different purity efficiencies obtained as a function of the entrance hematocrit levels in the 20 μm plasma channel microfluidic chip. Some hematocrit levels have several experimental points (two or four). Two points are due to the independent measurement of data from each plasma outlet. Four points are due to 100 g L^{-1} for sample of eHCT of 33.7% processed at 5 mL h^{-1} . Two different experiments, each of them having two different experimental points from each of the plasma outlets. Three different flow rates were used (2 mL h^{-1} , 5 mL h^{-1} and 10 mL h^{-1}), hence Fig. 3 also measures the influence of flow rate on the separation efficiencies. At entrance hematocrit (eHCT) levels of 1.8% to 10%, the efficiency of the first plasma branch is comprised between 95% and 100%. For an entrance hematocrit greater than 10% the purity efficiency decreases regularly from approximately 95% to 32% for an eHCT of 33.7%. Haemoglobin levels recorded by the Cell Counter Coulter are

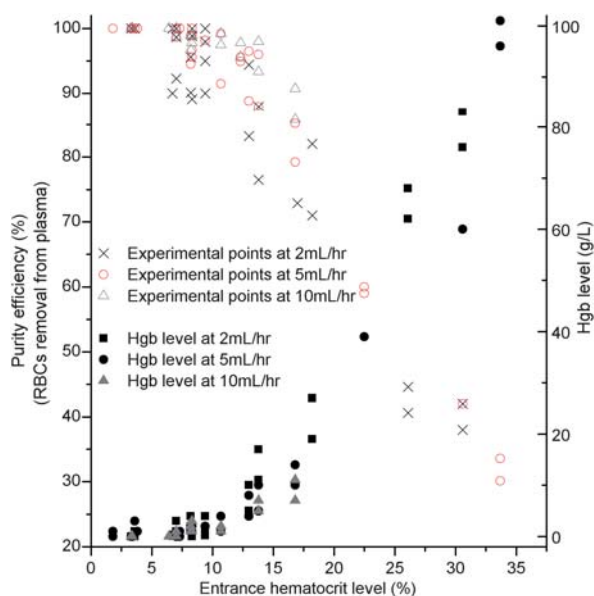


Fig. 3 Influence of the hematocrit level on the purity efficiency and cell lysis in the 20 μm wide plasma channels model at different blood flow rates.

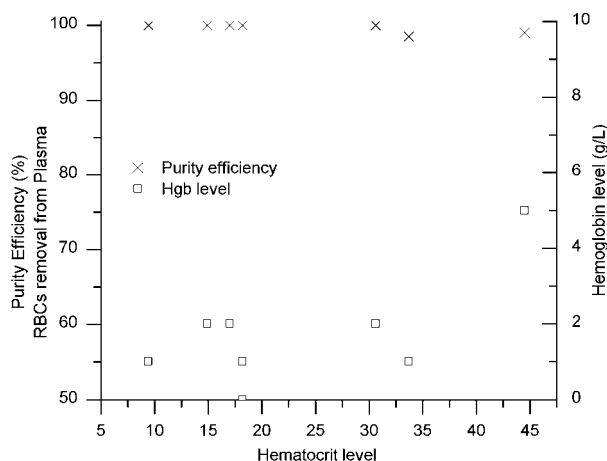


Fig. 4 Influence of the hematocrit level on the purity efficiency and cell lysis in the 10 μm wide plasma channels model for a flow rate of 2 mL h^{-1} .

also indicated here to report on the damage of the RBCs. Below eHCT of 15% the haemoglobin level is below 20 g L^{-1} . The total yield obtained by the 20 μm wide channel design was approximately 30%.

Fig. 4 details the results of the 10 μm plasma channel chips. In these experiments the only flow rate used was 2 mL h^{-1} . Again haemoglobin levels are indicated here to report on RBC damage. The haemoglobin levels are increasing with the hematocrit, but stay below the level reported to introduce interference with PCR reactions (5 g L^{-1}).⁵ The purity efficiency decreases very slightly (99%) towards hematocrit levels comparable to whole human blood, with plasma yield reaching 5%.

Hematocrit and the cell-free zones. The influence of the eHCT on the cell-free zone was observed independently of the flow rate at each bifurcation. Fig. 5 shows the dependence at bifurcation number 7 shown in Fig. 1, of the cell-free zone on the entrance hematocrit level (eHCT). The lower the entrance hematocrit level, the larger is the cell free zone. As illustrated in Fig. 5, the cell-free zone can be measured from the middle of the construction lateral dimension. From (a) to (b), the hematocrit is divided by 2, while the cell-free zone size is multiplied by 2.5. For low hematocrit levels (8.3% and 3.3%) and a relatively high flow rate (here 10 mL h^{-1}), a recirculation pattern forms just after the constriction, while no recirculation is observed for a level of 16.8%. The lower the hematocrit level, the larger the recirculation pattern will be. The recirculation does not affect the separation efficiency at this flow rate, nor does it indicate the presence of turbulence. A previous study has also shown that recirculations might be present at lower flow rate even if not visible, but found no proof they can enhance the separation.⁴⁵

Flow rate and the cell-free zones. In the same fashion, the influence of the flow rate on the cell-free zones has been observed. Three separation experiments were carried out with the same entrance hematocrit of 8.3% and varying flow rates of 2 mL h^{-1} , 5 mL h^{-1} and 10 mL h^{-1} . The effect of the flow rate at the third bifurcation is shown in Fig. 5 (d,e,f). Compared to the previous example, no recirculation eddies are observed at bifurcation number 3. The size of cell-free zone here is approximately linear relative to the flow rate. However, more data would be needed to

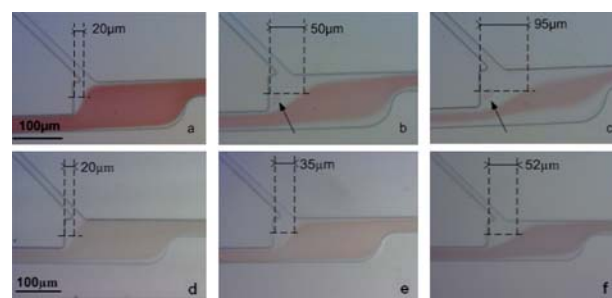


Fig. 5 Effect of the entrance hematocrit level at bifurcation 7 for a constant flow rate of 10 mL h^{-1} , at (a) eHCT = 16.8% (b) eHCT = 8.3% (c) eHCT = 3.3%. The arrow highlights the recirculation flow in (b) and (c). Effect of the flow rate at bifurcation 3, for an entrance HCT = 8.3% at (d) 2 mL h^{-1} (e) 5 mL h^{-1} (f) 10 mL h^{-1} . Note: the changes in colour are only due to camera settings at the time of the photograph.

establish this linearity. A high flow rate ultimately leads to a higher purity but also increases the risk of damaging the cells through greater shear rate forces.

Flow cytometric study

Motivation. A flow cytometric study was performed on several samples to get an in-depth knowledge of the separation of plasma from blood. Flow cytometry allows a very precise counting of particles in a fluid and, in this case, provides information on the cell population, such as cell lysis that may be caused by the high shear rates in the microchannels. Flow cytometry offers a higher level of sensitivity than can be achieved with a Coulter Counter. As the ultimate goal of the plasma separation is to detect cfDNA

in the plasma, it is crucial to prove that the cells are not damaged/destroyed during separation. Damaging the cells and causing lysis leads to more contamination of the plasma. In order to give useful biomedical information, the cfDNA detected in the plasma should be present in the blood prior to extraction and should not come from cell lysis as a result of sample preparation.

Results. Fig. 6 shows the results of the flow cytometric data after processing. The horizontal axis represents the size of the cells (Forward Scatter, FSC) and the vertical axis represents their granularity (Side Scatter, SSC). In the feed collection the population is mainly constituted of RBCs (95.62%), platelets (4.1%), leucocytes (0.28%), which corresponds to normal physiological conditions. Additionally the counting beads are present in the

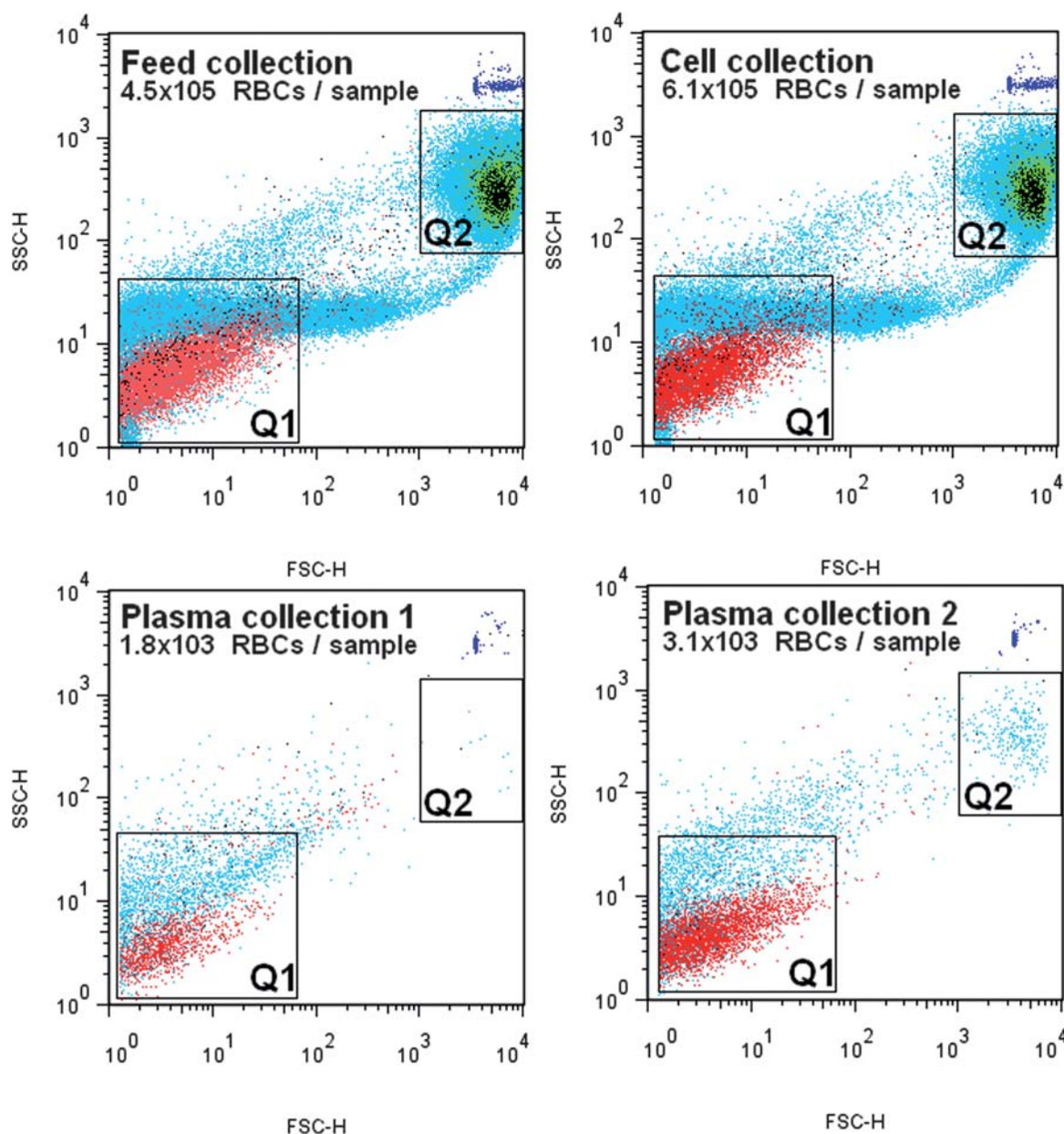


Fig. 6 Dot plots of FSC vs. SSC represent the acquisition of 1000 flow check beads in the 250 μ L feed, cell, plasma 1 and plasma 2 collections. Colour correspondence: Dark blue: Flow Check beads, Black: leukocytes, Red: platelets, Light Blue: RBCs, Green: monocytes-platelets or platelets aggregates.

mixture, as well as the population identified as platelets aggregates and platelets-monocytes aggregates.⁴⁶ The platelets are located in the bottom-left quadrant of the diagram, as they are the smallest and least granular particles. In this quadrant a large population of red blood cells is also present; these are either very small RBCs or RBCs debris present in the blood before separation. The presence of these debris can be explained by cell damage caused by the processing, transport and storage of the blood. Other RBCs, counting beads, monocytes and platelets aggregates can be found in the upper right quadrant. Linking these two quadrants is the “tail” of the healthy RBCs population, smaller or damaged RBCs. Little change is observed between the feed collection and the cell collection after separation. The tail does not show signs of growth which means that the cells either have not been through high stress or have resisted the stress. Looking at the plasma collection outlets, the plasma is not entirely devoid of cells, but has been strongly depleted by 250 times compared to the feed sample. Most of the RBCs debris has also been removed, which enhances the overall quality of the plasma. The population of platelets is the less depleted of all cell populations. This confirms the results from a previous study by Sollier *et al.*⁴⁵ Additionally a measurement of the potassium ion concentration could be used as a marker of cell death to assess global cell damage. This has not been carried out in this study.

In conclusion, the flow cytometric investigation has shown that the cells are not damaged through the system. Additionally, the plasma is not entirely devoid of cells as the cell coulter counter suggests, but the RBC population in the plasma collection has been reduced 250 times compared to the feed sample. Finally, the system also removes the cell debris, rendering the plasma even purer.

Detection of biomarkers

Of interest in this study is the subsequent recovery of cfDNA from the plasma after the on-chip blood plasma separation process. To assess the quality of the plasma extracted on-chip, PCR for a house-keeping gene was performed. The GAPDH gene was chosen for its small molecular weight, 200 bp which makes it a challenging target to amplify and also because its size is comparable to cfDNA fragments.⁴⁰ The goal of this biological study is to prove that cfDNA can be amplified and detected in plasma obtained using this on-chip separation method. In order to investigate whether the dilution level prior to separation alters the recovery of biomarkers we studied the influence of pre-dilution on the PCR efficiency. The influence of the separation efficiency on the PCR efficiency has also been measured to characterise the limits of the separation method.

Conventional PCR and gel electrophoresis on house-keeping genetic sequences

The theoretical aspect of PCR has already been treated in a large body of literature.^{47,48} PCR was performed using a Primus 96 thermal cycler. In order to assess the suitability of on-chip blood separation as a module in a larger μ TAS system with minimal processing steps, no further purification was carried out on the plasma prior to PCR.

Influence of the dilution of whole blood previous to on-chip separation

PCR was performed to detect the GAPDH gene in the plasma samples extracted on-chip. Samples were isolated after separation and stored in 1 mL eppendorf tubes at 4 °C prior to use. The separation efficiency was characterised by a Coulter Counter as described previously. In order to assess the influence of the dilution on the PCR efficiency, six samples with the same separation efficiency but different dilution levels (eHCT level varying from 3.3% to 33.7%) were chosen. Achieving the same separation efficiency with different pre-diluted samples is possible through the use of the two chip models and different flow rates.

PCR and gel electrophoresis were performed on 18 samples, following the protocol presented in the previous section. Samples S1 to S6 were duplicated to verify the consistency of the PCR results. Table 1 summarises the different samples and controls used in this experiment.

The amplified products of the plasma samples are shown in Fig. 7. In all columns except the one of the negative control, a clear 200 bp band is present, showing the consistent amplification of the GAPDH gene fragment. The intensity of the band varies from sample to sample, but does not vary within the duplicates. Both samples in series 1 show a relatively strong amplification band. Interestingly, there is a broad trend towards higher fluorescence signal from S1 to S6, (excluding S5) which confirms, as expected, that the resulting concentration achieved by PCR amplification depends on the entrance hematocrit of the sample. Additionally, the presence of an amplification band in the sample with the highest dilution, with corresponding hematocrit level 3.3%, demonstrates that PCR can be achieved on strongly diluted samples. All the other controls, including the negative controls show no amplification. For the lanes containing the whole blood product (WB), and the plasma extracted by centrifugation (C), the PCR has been inhibited, probably by the presence of immunoglobulin G in the whole blood and in the plasma sample extracted by centrifugation. One explanation for finding immunoglobulin in the latter sample can be found in the gentle parameters used for the centrifugation (3000 rpm, 10 min). To the best of our knowledge, this is the first demonstration of PCR on cfDNA in plasma extracted on chip.

Table 1 Characteristics of the samples and controls used in the blood dilution influence experiment

		Separation efficiency of sample (%)	Entrance hematocrit level (%)
Samples	S1	100	3.3
	S2	100	6.2
	S3	100	7.0
	S4	100	14.9
	S5	100	17
	S6	100	33.7
Positive controls	G1	<i>Genomic control 1 – 1/10</i>	
	G2	<i>Genomic control 2 – 1/100</i>	
	G3	<i>Genomic control 3 – 1/1000</i>	
Other controls	WB	<i>Whole blood</i>	
	C	<i>Plasma sample extracted by gentle centrifugation (3000 rpm, 10 min)</i>	
Negative control	W	<i>Ultrapure water</i>	

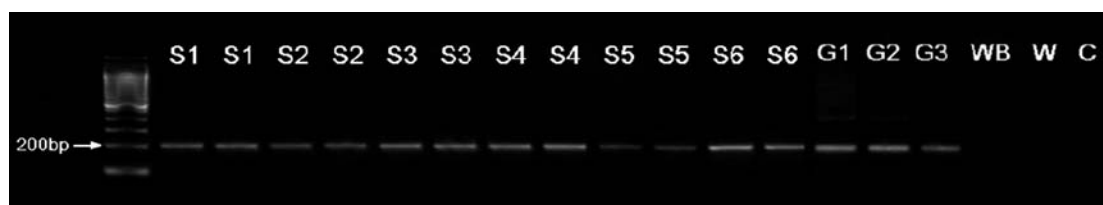


Fig. 7 Ethidium bromide-stained agarose gel of PCR products obtained with GAPDH primer and unprepared plasma samples obtained by microfluidic extraction. The first lane is a molecular weight marker (1000-bp ladder).

Influence of the separation efficiency on the PCR efficiency

As demonstrated by Fig. 7, PCR can be achieved on cfDNA in plasma extracted on-chip for purity efficiency of 100%. Further study was carried out to assess the limits of the PCR capability on cfDNA in untreated plasma sample. In that respect, plasma aliquots from samples with similar entrance hematocrit levels and with different purity efficiencies were collected after separation and stored at 4 °C. The different samples used in this experiment are presented in Table 2. The separation efficiency of the samples ranged from 65.1% to 100%.

The amplified products of this experiment are shown in ethidium bromide-stained agarose gel in Fig. 8. A clear gradient of band intensity through samples S1 to S5 can be observed. No PCR product could be amplified from S5 (purity 65.1%), whole blood and water lanes. The band from S4 (purity 84%) is visible but faint. This experiment demonstrates that the PCR efficiency

Table 2 Characteristics of the samples and controls used in the experiment on separation efficiency influence

		Separation efficiency (%)	Hematocrit level (%)
Plasma samples	S1	100	14.9
	S2	97.8	12.3
	S3	94.9	12.3
	S4	84	16
	S5	65.1	16
Positive controls	G1	<i>Genomic control 1 – 1/10</i>	
	G2	<i>Genomic control 2 – 1/100</i>	
	G3	<i>Genomic control 3 – 1/1000</i>	
Other control	WB	<i>Whole blood control</i>	
Negative control	W	<i>Ultrapure water</i>	

depends on the separation efficiency, and most importantly shows that at the high separation efficiencies which are standard for our device, PCR can be routinely performed. Moreover these experiments have successfully shown that the plasma extracted on-chip is pure enough to perform amplification without further purification steps as routinely done after centrifugation today, reducing thereby reagent costs, material waste and processing time. For more difficult cfDNA targets such as cfDNA, this step might still be necessary.

One final and important point to consider is the effect of the time delay between draw and processing of blood which has been shown to be a factor in the quantification of cfDNA. Lysis of intact cells caused by a delay in blood processing would result in increased concentrations of cfDNA (caused by *ex-vivo* processing) which might lead to misleading results especially if cfDNA is used as a biomarker in cancer, prenatal and post transplant care. Integrating the process of blood plasma separation and PCR analysis onto a single chip will overcome this limitation for the routine use of cfDNA analysis in clinical settings.

Conclusions

This paper demonstrates an efficient and disposable way to extract at high flow rate cell-free plasma from whole blood at different dilution levels. The purity efficiency reached 100% even with the use of relatively large channels (20 μm) which are suitable for mass manufacturing. PCR was used to demonstrate the purity of the extracted plasma without the need for DNA extraction. To the best of our knowledge, we describe for the first time the recovery of cell-free DNA from on-chip extracted plasma by PCR and gel electrophoresis. As expected, the detection of nucleic acids biomarker depends on the separation

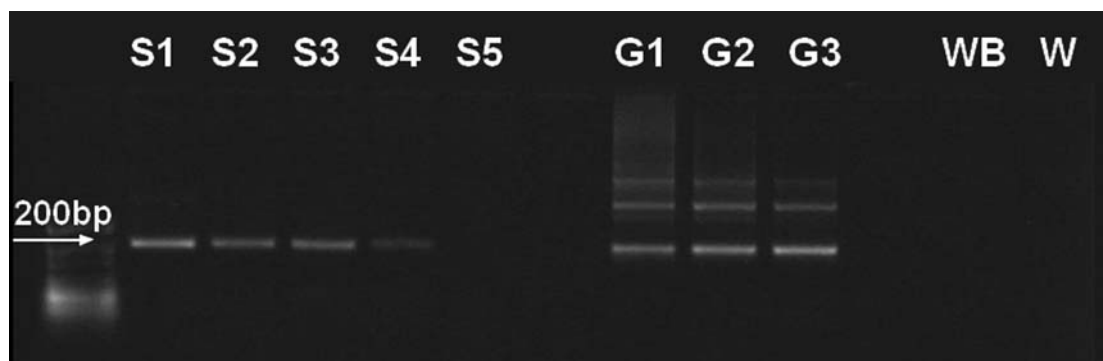


Fig. 8 Influence of the separation efficiency on the detection of the GapDH house-keeping gene in the on-chip extracted plasma. The first lane is a molecular weight marker (50-bp ladder).

efficiency, but also on the dilution of the blood. Detection was demonstrated in plasma samples with purity efficiency down to 84% and dilution level up to 1 : 20. All our findings indicate that this continuous microfluidic separation system may be used as a preliminary module for a lab-on-chip system.

Acknowledgements

The staff of the Division of Pathway Medicine, University of Edinburgh is thanked for their help in the preparation of the PCR reactions. We would like to thank Neil Johnston for access to the Centre for Cardiovascular Science, Queen's Medical Research Institute, Edinburgh, for cell counting. Shonna Johnston is thanked to allow access to the Flow Laboratory, Queen's Medical Research Institute, Edinburgh and for the provision of antibodies. Thank you to Tiina Kitari for providing flow check beads. Funding from the EPSRC 3DM-Integration Grand challenge project EP/C534212/1 is gratefully acknowledged. The manufacturing of the lab-on-a-chip was carried out by Epigem Ltd in the Fluence Microfluidics Application Centre supported by the Technology Strategy Board (TSB) and the ONE Regional Development Agency as part of the UK's MNT Network.

Notes and references

- 1 J. V. Zoval and M. J. Madou, *Proc. IEEE*, 2004, **92**, 140–153.
- 2 S. Haerberle, T. Brenner, R. Zengerle and J. Ducrée, *Lab Chip*, 2006, **6**, 776–781.
- 3 J. Siegrist, R. Gorkin, M. Bastien, G. Stewart, R. Peytavi, H. Kido, M. Bergeron and M. Madou, *Lab Chip*, 2010, **10**, 363–371.
- 4 J. Moorthy and D. J. Beebe, *Lab Chip*, 2003, **3**, 62–66.
- 5 V. Vandellinder and A. Groisman, *Anal. Chem.*, 2006, **78**, 3765–3771.
- 6 X. Chen, D. F. Cu, C. C. Liu and H. Li, *Sens. Actuators, B*, 2008, **130**, 216–221.
- 7 H. Becker, *Lab Chip*, 2010, **10**, 271–273.
- 8 E. Sollier, H. Rostaing, P. Pouteau, Y. Fouillet and J. L. Achard, *Sens. Actuators, B*, 2009, **141**, 617–624.
- 9 S. Yang, A. Ündar and J. D. Zahn, *Lab Chip*, 2006, **6**, 871–880.
- 10 R. Fan, O. Vermesh, A. Srivastava, B. K. H. Yen, L. Qin, H. Ahmad, G. A. Kwong, C.-C. Liu, J. Gould, L. Hood and J. R. Heath, *Nat. Biotechnol.*, 2008, **26**, 1373–1378.
- 11 M. Faivre, M. Abkarian, K. Bickraj and S. Howard, *Biorheology*, 2006, **43**, 147–159.
- 12 D. Di Carlo, J. F. Edd, D. Irimia, R. G. Tompkins and M. Toner, *Anal. Chem.*, 2008, **80**, 2204–2211.
- 13 A. I. Rodríguez-Villarreal, M. Arundell, M. Carmona and J. Samitier, *Lab Chip*, 2010, **10**, 211–219.
- 14 Y. Nakashima and T. Yasua, *Proc. of μ TAS*, 2007, 706–708; A. Lenshof, A. Ahmad-Tajudin, K. Järäs, A. M. Swärd-Nilsson, L. Aberg, G. Marko-Varga, J. Malm, H. Lilja and T. Laurell, *Anal. Chem.*, 2009, **81**, 6030–6037; M. Takayasu, D. R. Kelland and J. V. Minervini, *IEEE Trans. Appl. Supercond.*, 2000, **10**, 927–930.
- 15 M. Kersaudy-Kerhoas, R. S. Dhariwal, M. P. Y. Desmulliez and L. Jouvet, *Microfluid. Nanofluid.*, 2010, **8**, 105–114.
- 16 *Br. Pat.*, IPO 310809, 2009.
- 17 S. A. Leon, B. Shapiro, D. M. Sklaroff and M. J. Yaros, *Cancer Res.*, 1977, **37**, 646–650.
- 18 H. Schwarzenbach, C. Alix-Panabières, I. Müller, N. Letang, J. P. Vendrell, X. Rebillard and K. Pantel, *Clin. Cancer Res.*, 2009, **15**, 1032–1038.
- 19 O. Gautschi, C. Bigosch, B. Huegli, M. Jermann, A. Marx, E. Chasse, D. Ratschiller, W. Weder, M. Joeger, D. C. Betticher, R. A. Stahel and A. Ziegler, *J. Clin. Oncol.*, 2004, **22**, 4157–4164.
- 20 M. Fleischhacker and B. Schmidt, *Biochim. Biophys. Acta*, 2007, **1775**, 181232.
- 21 F. Diehl, M. Li, D. Dressman, Y. He, D. Shen and S. Szabo, *et al.*, *Proc. Natl. Acad. Sci. U. S. A.*, 2005, **102**, 16368–16373.
- 22 B. Shapiro, M. Chakrabarty, E. M. Cohn and S. A. Leon, *Cancer*, 1983, **51**, 2116.
- 23 V. Garcia Moreira, B. Prieto García, J. M. Baltar Martín, F. Ortega Suárez and F. V. Alvarez, *Clin. Chem.*, 2009, **55**, 1958–1966.
- 24 Y. M. D. Lo, *J. Histochem. Cytochem.*, 2005, **53**, 293.
- 25 J. M. Costa and P. Ernault, *Clin. Chem.*, 2002, **48**, 679.
- 26 K. M. Finning, P. G. Martin, P. W. Soothill and N. D. Avent, *Transfusion*, 2002, **42**, 1079.
- 27 C. Wright, PHG Foundation, 2009, <http://www.phgfoundation.org/pages/ffdna.html>.
- 28 X. Y. Zhong, W. Holzgreve and S. Kahn, *Hypertens. Pregnancy*, 2002, **21**, 77.
- 29 S. Jahr, H. Hentze, S. Englisch, D. Hardt, F. O. Fackelmayer, R. D. Hesch and R. Knippers, *Cancer Res.*, 2001, **61**, 1659–1665.
- 30 A. Sekizawa, M. Jimbo, H. Saito, M. Iwasaki, Y. Sugito and Y. Yukimoto, *et al.*, *Clin. Chem.*, 2002, **48**, 353–354.
- 31 Y. Ohashi, N. Mihar, H. Honda, O. Samura and K. Ohama, *Clin. Chem.*, 2002, **48**, 386–388.
- 32 E. K. Ng, N. B. Tsui, T. K. Lau, T. N. Leung, R. W. Chiu and N. S. Panesar, *et al.*, *Proc. Natl. Acad. Sci. U. S. A.*, 2003, **100**, 4748–4753.
- 33 P. Anker and M. Stroun, *Medicina (B Aires)*, 2000, **60**, 699–702.
- 34 M. Stroun, P. Anker, J. Lyautey, C. Lederrey and P. A. Maurice, *Eur. J. Cancer Clin. Oncol.*, 1987, **23**, 707–712.
- 35 H. D. Halicka, E. Bedner and Z. Darzynkiewicz, *Exp. Cell Res.*, 2000, **260**, 248–256.
- 36 Y. M. D. Lo, M. S. Tein, T. K. Lau, C. J. Haine, T. N. Leung and P. M. Poon, *Am. J. Hum. Genet.*, 1998, **62**, 768.
- 37 D. W. Bianchi, *Trophoblast Research*, 2004, **18**, S93–S101.
- 38 A. W. Al-Soud, L. J. Jönsson and P. Rådström, *J. Clin. Microbiol.*, 2000, **38**, 345–350.
- 39 R. W. K. Chiu, L. L. M. Poon, T. K. Lau, T. N. Leung, E. M. C. Wong and Y. M. D. Lo, *Clin. Chem.*, 2001, **47**, 1607–1613.
- 40 X. Xue, M. D. Teare, I. Hølen, Y. M. Zhu and P. J. Woll, *Clin. Chim. Acta*, 2009, **404**, 100–104.
- 41 B. Schmidt, S. Weickmann, C. Witt and M. Fleischhacker, *Clin. Chem.*, 2005, **51**, 1561–1563.
- 42 G. Sitar, L. Manenti, A. Farina, V. Lanati, P. Mascheretti, A. Forabosco, L. Montanari and E. Ascari, *Haematologica*, 1997, **82**, 5.
- 43 Y. C. Fung, in *Biomechanics*, 2004, Springer.
- 44 S. S. Shevkopyas, S. C. Gifford, T. Yoshida and M. W. Bitensky, *Microvasc. Res.*, 2003, **65**, 132–136.
- 45 E. Sollier, M. Cubizolles, M. Faivre, Y. Fouillet and J. L. Achard, *Proc. IEEE Eng. Med. Biol. Soc.*, 2009, **1**, 7030–7033.
- 46 Y. Yoshimura, Y. Hiramatsu, Y. Sato, S. Homma, Y. Enomoto, Y. Kikuchi and Y. Sakakibara, *Ann. Thorac. Surg.*, 2003, **75**, 1254–1260.
- 47 D. G. Remick, S. L. Kunkel and E. A. Holbrook, *et al.*, *Am. J. Clin. Pathol.*, 1990, **93**, S49–S54.
- 48 P. A. Wright and D. Wynfordthomas, *J. Pathol.*, 1990, **162**, 99–117.